Where do the AMS-02 antihelium events come from?

Vivian Poulin, Pierre Salati, Ilias Cholis, Marc Kamionkowski, Joseph Silk

Where do the *AMS-02* antihelium events come from?

Vivian Poulin,[1] Pierre Salati,[2] Ilias Cholis,[3,1] Marc Kamionkowski,[1] and Joseph Silk[1,4,5]

[1]*Department of Physics and Astronomy, Johns Hopkins University, Baltimore, Maryland 21218, USA*
[2]*LAPTh, Université Savoie Mont Blanc & CNRS, 74941 Annecy Cedex, France*
[3]*Department of Physics, Oakland University, Rochester, Michigan 48309, USA*
[4]*Sorbonne Universités, UPMC Univ. Paris 6 et CNRS, UMR 7095, Institut dAstrophysique de Paris, 98 bis bd Arago, 75014 Paris, France*
[5]*Beecroft Institute of Particle Astrophysics and Cosmology, Department of Physics, University of Oxford, Denys Wilkinson Building, 1 Keble Road, Oxford OX1 3RH, United Kingdom*

(Received 17 September 2018; published 28 January 2019)

We discuss the origin of the antihelium-3 and -4 events possibly detected by *AMS-02*. Using up-to-date semianalytical tools, we show that spallation from primary hydrogen and helium nuclei onto the ISM predicts a $\overline{^3\mathrm{He}}$ flux typically one to two orders of magnitude below the sensitivity of *AMS-02* after 5 years, and a $\overline{^4\mathrm{He}}$ flux roughly 5 orders of magnitude below the *AMS-02* sensitivity. We argue that dark matter annihilations face similar difficulties in explaining this event. We then entertain the possibility that these events originate from antimatter-dominated regions in the form of anticlouds or antistars. In the case of anticlouds, we show how the isotopic ratio of antihelium nuclei might suggest that BBN has happened in an inhomogeneous manner, resulting in antiregions with a antibaryon-to-photon ratio $\bar{\eta} \simeq 10^{-3}\eta$. We discuss properties of these regions, as well as relevant constraints on the presence of anticlouds in our Galaxy. We present constraints from the survival of anticlouds in the Milky-Way and in the early Universe, as well as from CMB, gamma-ray and cosmic-ray observations. In particular, these require the anticlouds to be almost free of normal matter. We also discuss an alternative where antidomains are dominated by surviving antistars. We suggest that part of the unidentified sources in the 3FGL catalog can originate from anticlouds or antistars. *AMS-02* and *GAPS* data could further probe this scenario.

DOI: 10.1103/PhysRevD.99.023016

I. INTRODUCTION

The origin of cosmic ray (CR) antimatter is one of the many conundrums that *AMS-02* is trying to solve thanks to precise measurements of CR fluxes at the Earth. In over six years, *AMS-02* has accumulated several billion events, whose composition is mostly dominated by protons and helium nuclei. Moreover, positrons and antiprotons have been frequently observed and are the object of intense theoretical investigations in order to explain their spectral features. Indeed, antimatter particles are believed to be mainly of secondary origin, i.e., they are created by primary CR nuclei (accelerated by supernova-driven shock waves) impinging onto the interstellar medium (ISM). However, deviations from these standard predictions have been observed, hinting at a possible primary component. In the case of positrons, a very significant high-energy excess has already been seen in *PAMELA* data [1]. The main sources under investigation to explain this excess are DM and pulsars (see e.g., [2–26]). In the case of antiprotons, a putative excess at the GeV-energy [27] is under discussion [28]. Still, antiprotons represent one of the most promising probes to look for the presence of DM in our Galaxy through its annihilation.

But the searches for antimatter CR do not limit themselves to antiprotons and positrons. Hence, many theoretical and experimental efforts are devoted to detecting antideuterons, which are believed to be a very clean probe of DM annihilations especially at the lowest energies (below tens of GeV) [29–32]. Similarly, measurement of the anti-helium nuclei CR flux is a very promising probe of new physics, that has been suggested to look for DM annihilations [31,33–35] or other sources of primary CR, such as antimatter stars or clouds [36–38]. Strikingly, *AMS-02* has recently reported the possible discovery of eight antihelium events in the mass region from 0 to 10 GeV/c^2 with $Z = 2$ and rigidity < 50 GV [39]. Six of the events are compatible with being antihelium-3 and two events with antihelium-4. The total event rate is roughly one antihelium in a hundred million heliums. This preliminary sample includes one event with a momentum of 32.6 ± 2.5 GeV/c and a mass of 3.81 ± 0.29 GeV/c^2 compatible with that of antihelium-4. Earlier already, another event with a momentum of 40.3 ± 2.9 GeV and a mass compatible with antihelium-3 had been reported [40].

In this paper, we discuss various possibilities for the origin of *AMS-02* anti-helium events. Should these events be

confirmed, their detection would be a breakthrough discovery, with immediate and considerable implications onto our current understanding of cosmology. The discovery of a single antihelium-4 nucleus is challenging to explain in terms of known physics. In this article, we start stressing why such a discovery is unexpected. For this, we reevaluate the secondary flux of antihelium nuclei. In particular, we provide the first estimate of the $\overline{^4\mathrm{He}}$ flux at the Earth coming from the spallation of primary CR onto the ISM. We show that it is impossible to explain AMS results in terms of a pure secondary component, even though large uncertainties still affect the prediction. Moreover, we argue that the DM explanations of these events face similar difficulties, although given the virtually infinite freedom in the building of DM models, it is conceivable that a tuned scenario might succeed in explaining these events.

We then discuss the implications of the antihelium observation. We essentially suggest that the putative detection of $\overline{^3\mathrm{He}}$ and $\overline{^4\mathrm{He}}$ by *AMS-02* indicates the existence of an anti-world, i.e., a world made of antimatter, in the form of antistars or anticlouds. We discuss properties of these regions, as well as relevant constraints on the presence of anticlouds in our Galaxy. We present constraints from the survival of anticlouds in the Milky Way and in the early Universe, as well as from CMB, gamma-ray and cosmic-ray observations. We show in particular that these require the anticlouds to be almost free of normal matter. Moreover, we show how the isotopic ratio of antihelium nuclei might suggest that BBN happened inhomogeneously, resulting in antiregions with a antibaryon-to-photon ratio $\bar{\eta} \simeq 10^{-3}\eta$. Given the very strong constraints applying to the existence and survival of anticlouds, we also discuss an alternative scenario in which antidomains are dominated by antistars. We suggest that part of the unidentified sources in the 3FGL catalog can be anticlouds or antistars. Future *AMS-02* and *GAPS* data could further probe this scenario.

The paper is structured as follows. Section II is devoted to a thorough reevaluation of the secondary astrophysical component from spallation within the coalescence scheme. A discussion on the possible limitations of our estimates and on the DM scenario is also provided. In Sec. III, we discuss the possibility of antidomains in our Galaxy being responsible for *AMS-02* events. Properties of anticlouds and their constraints are presented in Sec. III A, while the alternative antistar scenario is developed in Sec. III B. Finally, we draw our conclusions in Sec. IV.

II. UPDATED CALCULATION OF $\bar{d}$, $\overline{^3\mathrm{He}}$ AND $\overline{^4\mathrm{He}}$ FROM SPALLATION ONTO THE ISM

As for any secondaries, the prediction of the $\overline{^3\mathrm{He}}$ flux at Earth is the result of two main processes affected by potentially large uncertainties: (i) the *production* due to spallation of primary CR onto the ISM and (ii) the *propagation* of cosmic rays in the magnetic field of our Galaxy, eventually modulated by the impact of the Sun. In this section, we briefly review how to calculate the secondary flux of $\overline{^3\mathrm{He}}$ from spallation onto the ISM in a semianalytical way.

A. Source term for antinuclei in the coalescence scenario

The spallation production cross section of an antinucleus A from the collision of a primary CR species i onto an ISM species j can be computed within the *coalescence scenario* as follows:

$$\frac{E_A}{\sigma_{ij}}\frac{d^3\sigma_A^{ij}}{d^3k_A} = B_A \cdot \left(\frac{E_p}{\sigma_{ij}}\frac{d^3\sigma_p^{ij}}{d^3k_p}\right)^Z \cdot \left(\frac{E_n}{\sigma_{ij}}\frac{d^3\sigma_n^{ij}}{d^3k_n}\right)^{A-Z}, \quad (1)$$

where σ^{ij} is the total inelastic cross section for the ij collision, and the constituent momenta are taken at $k_p = k_n = k_A/A$. B_A is the coalescence factor, whose role is to capture the probability for A antinucleons produced in a collision to merge into a composite antinucleus. It is often written as

$$B_A = \left(\frac{4\pi}{3}\frac{p_{\mathrm{coal}}^3}{8}\right)^{A-1}\frac{m_A}{m_p^Z m_n^{A-Z}}, \quad (2)$$

where p_{coal} is the diameter of a sphere in phase-space within which antinucleons have to lie in order to form an anti-nucleus. The coalescence factor B_A is a key quantity which can be estimated from pp-collision data, as has been done recently by the ALICE collaboration [41] for antideuteron and antihelium. We use the values measured at low transverse momentum as these are adequate for CR spallation, namely $B_2 \simeq (15 \pm 5) \times 10^{-2}$ GeV^2 and $B_3 \simeq (2 \pm 1) \times 10^{-4}$ GeV^4. We extrapolate these values to pA and AA collisions. There is no measurement of B_4 yet available. Hence, we make use of Eq. (2) in order to extract the coalescence momentum (common to each species in the coalescence model) from the B_3 measurement. This gives a coalesence momentum that varies between 0.218 GeV and 0.262 GeV. Using the measurement of B_2, the coalescence momentum varies between 0.208 GeV and 0.262 GeV, which is in excellent agreement with the value extracted from B_3. We stress that the fact that the coalescence momenta extracted from both coalescence factors agree is far from trivial. It indicates that the coalescence scenario is much more predictive and accurate than one might have naively expected from its apparent simplicity. To phrase this otherwise: from the B_2 measurement of ALICE, one can predict how many antihelium-3 ALICE should measure; this turns out to be in very good agreement with the actual measurement, which is quite remarkable. The final step is thus to apply Eq. (2) to the case of antihelium-4. We find that B_4 varies between 7.7×10^{-7} GeV^6 and 3.9×10^{-6} GeV^6.

In the context of antiproton production, it has been found that [42]

$$E_n \frac{d^3\sigma_n^{ij}}{d^3k_n} = \Delta_{np} E_p \frac{d^3\sigma_p^{ij}}{d^3k_p}, \tag{3}$$

where $\Delta_{np} \simeq 1.3$ is introduced to model the isospin symmetry breaking. However, the ALICE experiment has extracted B_2 and B_3 assuming a perfect isospin symmetry between the antineutron and antiproton production. Hence, it would be wrong to make use of the factor 1.3 in this context and we set $\Delta_{np} = 1$. Additionally, we follow Ref. [29] and compute the antideuterium production cross section by evaluating the production cross sections of the two antinucleons at respectively $\sqrt{s}$ and $\sqrt{s} - 2E_p^*$ where E_p^* denotes the antinucleon energy in the center of mass frame of the collision. Similarly, for the antihelium-3 and -4 we evaluate cross sections decreasing the available center of mass energy $\sqrt{s}$ by $2E_p^*$ for each subsequent produced antinucleon. This ansatz has the merit of imposing energy conservation, although others are possible (see the discussion in Ref. [29]). We checked that adopting the other prescription $\sqrt{s} - m_p - E_p$ suggested in Ref. [29] does not affect our conclusions. Another possibility to extend the coalescence analysis down to near-threshold collision energies is to introduce an interpolating factor R in the RHS of Eq. (1) as suggested, e.g., in [43,44]. The secondary source term can then be readily computed as:

$$Q_{\rm sec}^{ij}(E_A) = 4\pi n_j \int_{E_{\rm th}}^{\infty} dE_i \phi_i(E_i) \frac{d\sigma_A^{ij}}{dE_A}(E_i, E_A), \tag{4}$$

with

$$\frac{d\sigma_A^{ij}}{dE_A} = 2\pi k_A \int_{-1}^{1} \left\{ E_A \frac{d^3\sigma_A^{ij}}{d^3k_A} \right\} d(-\cos\theta). \tag{5}$$

We assume the density of target hydrogen and helium in the ISM n_j to be 0.9 g/cm^3 and 0.1 g/cm^3 respectively and make use of the demodulated flux of hydrogen and helium from *AMS-02* with Fisk potential 730 MV. To calculate the contribution of the main channel $p + p \to \bar{A} + X$, we make use of the recent $p + p \to \bar{p} + X$ cross section parametrization from Ref. [42]. In order to incorporate other production channels (i.e., from spallation of and onto ^{4}He), we make use of scaling relations derived in Ref. [45] and multiply the $p + p \to \bar{p} + X$ cross section by $(A_T A_P)^{2.2/3}$ where A_P and A_T are the nucleon numbers of the projectile and target nuclei. The result of our computation is plotted in Fig. 1. A nice feature of the coalescence scenario is that it naturally predicts, for simple kinematic reasons, a hierarchical relation between the flux of $\bar{p}$, $\bar{d}$, $\overline{^3\mathrm{He}}$ and $\overline{^4\mathrm{He}}$, where each subsequent nucleus gets suppressed by a factor 10^{-4}–10^{-3}.

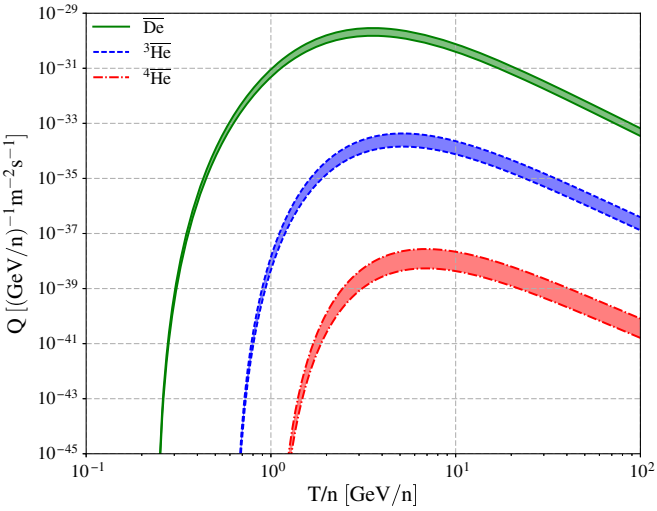

FIG. 1. Local source term for the secondary production of $\bar{d}$, $\overline{^3\mathrm{He}}$ and $\overline{^4\mathrm{He}}$. The width of the prediction represents the uncertainty on the coalescence parameter B_A.

B. Propagation in the Galaxy

To deal with propagation, we adapt the code developed in Refs. [46,47]. We model the Galaxy as a thin disk embedded in a 2D cylindrical (turbulent) magnetic halo and solve semianalytically the full transport equation for a charged particle. We include all relevant effects, namely diffusion, diffusive reacceleration, convection, energy losses, $\bar{\rm A}$ annihilation and tertiary production. The equation governing the evolution of the energy and spatial distribution function f of any species reads

$$\partial_t f + \partial_E\{b(E,\vec{x})f - K_{EE}(E)\partial_E f\} + \partial_z\{\mathrm{sign}(z) f V_c\} - K(E)\nabla^2 f = Q_{\rm II} + Q_{\rm III} - 2h\delta(z)\Gamma_{\rm ann} f. \tag{6}$$

We choose a homogeneous and isotropic diffusion coefficient $K(E) = \beta K_0 (R(E)/1\mathrm{GV})^\delta$ where β is the velocity of the particle and $R = p/(Ze)$ its rigidity, the ratio between the momentum $p = \sqrt{E^2 - m_A^2}$ and electric charge Ze. The diffusive reacceleration coefficient is expressed as $K_{EE}(E) = (2v_a^2 E^2 \beta^4)/(9K(E))$ where v_a is the drift—or Alfvèn—velocity of the diffusion centers. The (subdominant) energy losses are taken only in the disk $b(e,\vec{x}) = 2h\delta(z)b(E)$ where $h = 100$ pc is the half-height of the disk and include ionization, Coulomb and adiabatic losses. The gradient of V_c represents the convective wind, pushing outwards CR nuclei with respect to the disk. Possible annihilations of anti-nuclei A in the disk are encoded in the last term on the RHS of Eq. (6). The annilation rate takes the form $\Gamma_{\rm ann} = (n_{\rm H} + 4^{2.2/3} n_{\rm He}) v \sigma_{\rm ann}$, where $\sigma_{\rm ann}$ is the inelastic annihilation cross section. To estimate the deuteron annihilation cross section, we make use of the parametrization of the total cross section of $\overline{\rm H}d$ from Ref. [48] from which we

remove the nonannihilating contribution using a measurement presented in Ref. [31], that is $\sigma^{\bar{d}\mathrm{H}}_{\mathrm{no-ann}} = 4$ mb. This nonannihilation contribution is also used to calculate the tertiary source term Q_{III} following Ref. [46]. Our prescription for annihilation and tertiary is in very good agreement with that presented in Ref. [31]. To calculate the annihilation and tertiary production of anti-helium-3 and 4, we rescale all cross sections by a factor $(A/2)^{2.2/3}$. We treat the solar modulation in the force field approximation, setting the Fisk potential to 0.730 GV, the average value over AMS02 data taking period [49]. Our secondary predictions of antideuteron, antihelium-3 and -4 fluxes $\phi = \beta c f/(4\pi)$ are plotted in Fig. 2. We also show the antiproton flux associated to the same cross section and propagation parameters, in order to illustrate the relative amount of each antispecies from secondary production in our Galaxy. However, we stress that our secondary prediction for antiproton *is not* the most up-to-date one and can be within 50% of the most recent calculation done in Ref. [28]. We thus implemented the antiproton cross section parametrization from Ref. [28] and checked that it does not affect our conclusions regarding antideuteron and antihelium. We also checked that the impact of a break in the diffusion coefficient, as advocated in Refs. [28,50] from an analysis of the recent *AMS-02* proton, helium and B/C data, is negligible in the energy range we are interested in. Similarly, changing the value of the Fisk potential does not affect our prediction above a few GeV per nucleon.

In Fig. 3 we show the secondary prediction on anti-helium-3 and -4 compared to the advocated sensitivity of *AMS-02* after 5 years [51]. In principle, we should compare our prediction to the measured flux, but this one is not available. Still, we can deduce from the claimed ratio of $\overline{\mathrm{He}}/\mathrm{He} \sim 10^{-8}$ that this flux is larger by a factor of $\sim$10

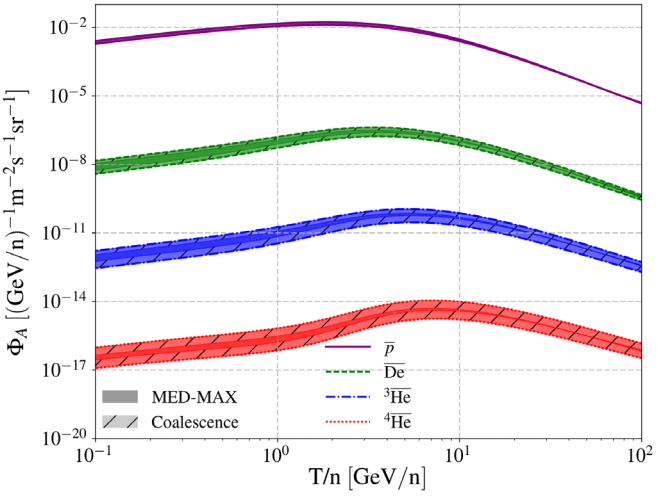

FIG. 2. Predicted secondary flux of $\bar{p}$, $\bar{d}$, $^3\overline{\mathrm{He}}$ and $^4\overline{\mathrm{He}}$ showing the uncertainty associated to the propagation and the coalescence momentum.

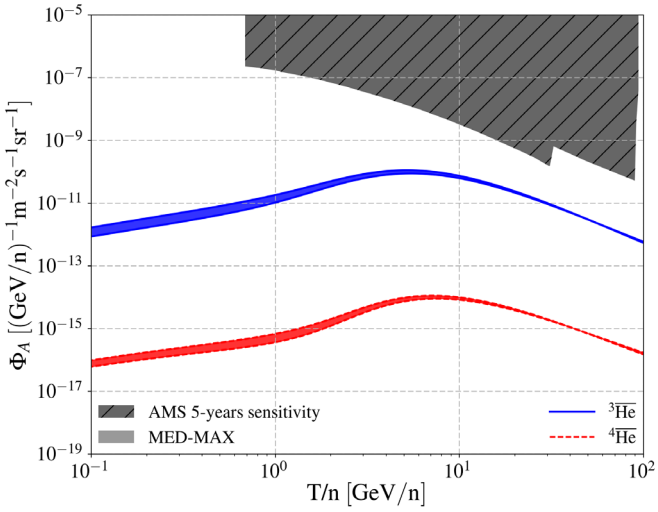

FIG. 3. Predicted secondary flux of $^3\overline{\mathrm{He}}$ and $^4\overline{\mathrm{He}}$ using the upper limit on the coalescence momentum deduced from the ALICE experiment and showing the uncertainty associated to the MED to MAX propagation model from Ref. [53]. We also show the expected sensitivity from *AMS-02* [51].

than the advocated sensitivity of *AMS-02* after 5 years around 10 GeV. Hence, we confirm that it is very challenging to explain the potential AMS02 anti-He signal as a pure secondary component. The $^3\overline{\mathrm{He}}$ is typically one to two orders of magnitude below the sensitivity of *AMS-02* after 5 years, and the $^4\overline{\mathrm{He}}$ is roughly 5 orders of magnitude below *AMS-02* sensitivity. Our results are in very good agreement with Ref. [52], who also found that the secondary prediction is, at best, roughly an order of magnitude below the tentative detection. Reference [44] on the other hand, concluded that a pure secondary explanation of the $^3\overline{\mathrm{He}}$ events was still viable. The main difference with Ref. [44] lies in the range of values considered for the coalescence momentum. As the analysis of Ref. [44] was completed, the Alice experiment had not yet published updated values for the coalescence factor of anti-helium B_3. Hence, the considered uncertainty range considered by Ref. [44] is much broader (up to 20×10^{-4} GeV^4) than the one considered in this work. When considering similar values of B_3, our results are in good agreement, even though the propagation of cosmic rays is treated in very different manners.

C. Boosting the production by spallation

Given the uncertainty on the mass measurement, it is conceivable that all of the antihelium nuclei are actually $^3\overline{\mathrm{He}}$ isotopes. The standard $^3\overline{\mathrm{He}}$ calculation yields a flux that is a factor $\sim$30–100 below what is measured by *AMS-02*. While uncertainties in the propagation are unlikely to be responsible for such mismatch, one might argue that the production term from spallation is underestimated. In order

to boost the secondary flux, one needs to increase the coalescence factor B_3 by the same amount. The ALICE experiment has reported a measurement of the coalescence factor from pp-collision with center of mass energies of 0.9 to 7 TeV instead of the few hundreds of GeV at which collisions occur in the ISM. It is conceivable that the B_3 factor differs at lower energies. However, there are several arguments going against a large increase of the coalescence factor at low energy:

(i) To commence, within the range of energies considered by ALICE (which spans an order of magnitude), the coalescence factor is very close to constant.

(ii) Then, there exist measurements [54] of the B_2 and B_3 factors from heavy ion collisions with beam energies between 0.4 and 2.1 GeV/nuc. Albeit probed at a much lower center-of-mass energy than in the case of ALICE, the coalescence momentum is found to lie in the range 0.173–0.304 GeV for deuterium and 0.130–0.187 GeV for tritium and helium-3. In the latter case, $p_{\rm coal}$ is smaller than what is found by ALICE at LHC energies. Our prediction for the production of $\overline{^3\mathrm{He}}$ in primary CR collisions onto the ISM tends to overestimate the actual rate.

(iii) Finally, from a theoretical perspective, we expect the rate of coalescence of nucleons to be higher at high energy than at low energy. Indeed, the collision of a high energy particle (having a large Lorentz boost) will create a jet of particles whose opening angle is smaller than that of a low-energy collision. This in turn will increase the correlation of nucleons within the shower and thus the probability for nucleons to merge. Moreover, the production of many nucleons in low-energy collisions is strongly suppressed by the phase-space. This theoretical consideration is in good agreement with what has been found in recent Monte-Carlo simulation studies [55]. The coalescence momentum (and hence the coalescence factor) decreases with lower center of mass energy. Hence, using the value obtained from ALICE data leads to a conservative overestimation of the antinuclei secondary fluxes.

Alternatively, increasing the grammage[1] seen by primary CRs along their journey towards Earth would enhance the yields of secondary nuclei. However such a scenario would result in all secondaries being affected in a similar way. Given the very good agreement (at the ∼20% level) between the measurement of the $\bar{p}$ flux and its current best secondary estimate, a large increase in the grammage of our Galaxy is not realistic.

In conclusion, it seems to us extremely unlikely that a boosted production by spallation is responsible for such a large $\overline{^3\mathrm{He}}$ flux. Naturally, the presence of $\overline{^4\mathrm{He}}$ goes as well against this scenario.

D. A word on $\overline{^3\mathrm{He}}$ and $\overline{^4\mathrm{He}}$ from dark matter annihilation

A recent reanalysis of the $\overline{^3\mathrm{He}}$ yield from Galactic DM annihilation has been presented in Refs. [35,52]. The formalism is very similar to that of production by spallation, and the estimate of the DM source term depends as well on the knowledge of the coalescence momentum p_A previously introduced. Similarly to secondary production, one expects a hierarchical relation between the fluxes of $\bar{p}$, $\bar{d}$, $\overline{^3\mathrm{He}}$ and $\overline{^4\mathrm{He}}$. According to Refs. [35,52], if DM is responsible for *AMS-02* events, it seems unlikely to observe $\overline{^3\mathrm{He}}$ without seeing a single $\bar{d}$ or overshooting $\bar{p}$ data. One caveat to this argument is that the sensitivity of *AMS-02* to $\bar{d}$ might be (much) smaller than that to $\overline{^3\mathrm{He}}$ in some energy range [51]. Still, the possible presence of $\overline{^4\mathrm{He}}$ events is at odds with the DM scenario.

III. $\overline{^3\mathrm{He}}$ AND $\overline{^4\mathrm{He}}$ AS AN INDICATION FOR AN ANTIWORLD

Motivated by the $\overline{^3\mathrm{He}}$ and $\overline{^4\mathrm{He}}$, in this section we discuss the possibility that extended regions made of antimatter have survived in our Galactic environment. There are many scenarios discussed in the literature and we present a few possibilities in Sec. IV. The two possible cases that regions of antimatter are present in our Galactic environment, are[2] (i) as ambient antimatter mixed with regular matter in the ISM or in the form of anticlouds; (ii) in the form of antistars. The presence of $\overline{^4\mathrm{He}}$, if confirmed, would be a hint at the presence of such antiregions. However, the fact that *AMS-02* measures more $\overline{^3\mathrm{He}}$ than $\overline{^4\mathrm{He}}$ (roughly 3∶1) is also interesting. As we discuss below, the isotopic ratio of antihelium can potentially carry information about the physical conditions (in particular antimatter and matter densities) within these regions.

A. Anticlouds

We argue that the presence of clouds of antimatter in our local environment can be responsible for the *AMS-02* events. We discuss properties of these clouds and constraints that apply to this scenario (in particular from nonobservation of γ-rays from matter-antimatter annihilation).

[1]The grammage measures the column density of interstellar matter crossed by CR. In an homogeneous and isotropic propagation model, it is directly proportional to the interstellar secondary flux.

[2]Additionally, compact objects might exist but would most likely not lead to the injection of high energy cosmic-rays and we therefore do not consider them here.

1. Exotic BBN as an explanation of the antihelium isotopic ratio

Standard big bang nucleosynthesis (BBN) predicts the presence of many more ^{4}He events, compared to ^{3}He. For normal matter, the isotopic ratio of ^{4}He:^{3}He is roughly $10^4:1$. Within CRs, the isotopic ratio is higher since ^{3}He can be produced through spallation of ^{4}He and, according to *PAMELA* [56], it reaches $\sim 5:1$ at a few GeV/n. Still, this is much lower than the possible measurement from *AMS-02*. As we have argued previously, increasing spallation by an order of magnitude is not realistic as it would affect all secondary species equally and lead to an overprediction of $\bar{p}$s.[3] Hence, inverting the isotopic ratio requires the presence of anisotropic BBN in regions where the (anti)-baryon-to-photon ratio strongly differs from that measured by *Planck* [57]. We therefore recalculated the BBN yields for a large number of η values using the BBN-code `AlterBBN`[4] [58] assuming *CP*-invariance for simplicity (Similar results are obtained with the BBN public code PRIMAT[5] [59]). We show in Fig. 4 the number density of $\overline{\mathrm{H}}$, $\overline{\mathrm{D}}$ and $\overline{^4\mathrm{He}}$ normalized to $\overline{^3\mathrm{He}}$ as a function of the (anti) baryon-to-photon ratio $\bar{\eta}$. The width of the band features the nuclear rate uncertainties.[6] It is possible then to obtain the right isotopic ratio (i.e., roughly $\overline{^4\mathrm{He}}:\overline{^3\mathrm{He}}$ of 1:3) for $\bar{\eta} \simeq 1.3$–6×10^{-13}. Interestingly, this also predicts the presence of non-negligible CR $\bar{p}$ and $\bar{d}$ fluxes that we comment on in Sec. III A 6. We also point out that while η from *Planck* refers to an average over the whole observable Universe, $\bar{\eta}$ is based on the isotopic ratio of $\overline{^4\mathrm{He}}:\overline{^3\mathrm{He}}$ and is therefore a local quantity. Depending on the object from which anti-helium events are originating, it is conceivable that this number varies from place to place even within our Galaxy such that *on average* the isotopic ratio of $\overline{^4\mathrm{He}}:\overline{^3\mathrm{He}}$ is as measured.

2. Some properties of the antidomains

We can get some information about the anticloud regions from the ratio $\phi_{\overline{\mathrm{He}}}/\phi_{\mathrm{He}}$ (integrated over all energies), assuming that it reflects the ratio of the abundance of $\overline{\mathrm{He}}$ to He in the ISM (i.e., acceleration and propagation of CR are identical for matter and antimatter), $N_{\overline{\mathrm{He}}}/N_{\mathrm{He}}$,

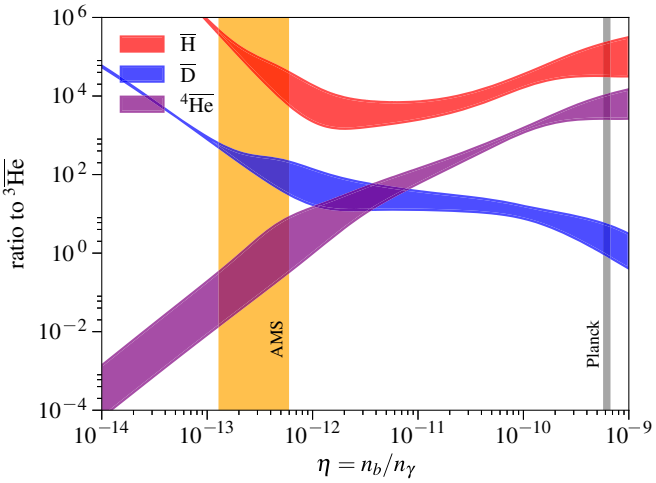

FIG. 4. Abundance of $\overline{\mathrm{H}}$, $\overline{\mathrm{D}}$ and $\overline{^4\mathrm{He}}$ with respect to that of $\overline{^3\mathrm{He}}$ as a function of the (anti)baryon-to-photon ratio $\bar{\eta}$. The *Planck* value is represented by the grey band. The value required by the *AMS-02* experiment is shown by the orange band.

$$\frac{\phi_{\overline{\mathrm{He}}}}{\phi_{\mathrm{He}}} \simeq \frac{N_{\overline{\mathrm{He}}}}{N_{\mathrm{He}}} \simeq \left(\frac{n_{\overline{\mathrm{He}}}}{n_{\bar{p}}}\right)\left(\frac{n_p}{n_{\mathrm{He}}}\right)\left(\frac{n_{\bar{b}}}{n_b}\right)\left(\frac{V_{\overline{\mathrm{M}}}}{V_{\mathrm{M}}}\right), \tag{7}$$

where $V_{\overline{\mathrm{M}}}$ and V_{M} represent the total volume of the antimatter and matter regions in our Galaxy. We have assumed here that $n_b = n_p$ which is correct at the 10% level and that $n_{\bar{b}} = n_{\bar{p}}$ that, as shown in Fig. 4 is also correct at better than the 10% level. The CR data can also tell us about some of these ratios: (i) $\phi_{\overline{\mathrm{He}}}/\phi_{\mathrm{He}}$ is of order $\sim 10^{-8}$; (ii) the ratio n_p/n_{He} is of order ~ 10; (iii) the ratio $n_{\overline{\mathrm{He}}}/n_{\bar{p}}$, from the BBN calculation motivated by the isotopic ratio $\overline{^4\mathrm{He}}:\overline{^3\mathrm{He}}$, is of order $\sim 10^{-5.5}$–10^{-4}. Hence we can get a constraint on the product of the total volume and density of these regions:

$$\left(\frac{n_{\bar{b}}}{n_b}\right)\left(\frac{V_{\overline{\mathrm{M}}}}{V_{\mathrm{M}}}\right) \sim 10^{-5}\text{–}10^{-3.5}. \tag{8}$$

It is possible to go one step further since the typical density of matter in the ISM is $n_b = 1\ \mathrm{cm}^{-3}$ and $V_{\mathrm{M}} = 2h\pi R_{\mathrm{gal}}^2 \sim 6 \times 10^{10}\ \mathrm{pc}^3$. Moreover, if we assume that antimatter forms spherical anticlouds of radius $r_{\bar{c}}$, we get $V_{\overline{\mathrm{M}}} = N_{\bar{c}}(4\pi/3r_{\bar{c}}^3)$ and derive

$$n_{\bar{b}} \simeq 10^5\text{–}10^{6.5} N_{\bar{c}}^{-1} \left(\frac{n_b}{1\ \mathrm{cm}^{-3}}\right)\left(\frac{r_{\bar{c}}}{1\ \mathrm{pc}}\right)^{-3} \mathrm{cm}^{-3}. \tag{9}$$

This key relation mostly relies on *AMS-02* data and knowledge about Galactic properties. The only theoretical assumption so far is that the isotopic ratio of antihelium is derived from BBN. From this we have additionally derived that at the time of BBN, $\bar{\eta}/\eta = n_{\bar{b}}/n_b \sim 10^{-3.5}$–$10^{-3}$. If this ratio still holds today, it would imply that there are $N_{\bar{c}} \sim 10^8$–$10^{10}(r_{\bar{c}}/1\ \mathrm{pc})^{-3}$ anticlouds in our Galaxy. The higher

[3] In Sec. III B, we estimate that this could be realistic close to compact objects such as antistars.

[4] https://alterbbn.hepforge.org

[5] http://www2.iap.fr/users/pitrou/primat.htm.

[6] A caveat is that nuclear uncertainty correlations are not provided. Hence, to calculate these bands, we simply vary all rates in the same way (increase them all or reduce them all simultaneously), i.e., we assume that all nuclear uncertainties are completely correlated, following the prescriptions implemented in ALTERBBN. This leads to the smallest uncertainty on the ratio and therefore a broader range of $\bar{\eta}$ values might in fact be allowed. A detailed study is left to future work.

end of $N_{\bar{c}}$ is close to the situation where the anticlouds are connected in the ISM. However, this probably strongly overestimates the number of such objects, as cosmological evolution can affect these regions (and in particular the ratio $n_{\bar{b}}/n_b$) compared to primordial conditions. More realistically, AMS measured events would originate from a few highly dense clouds.

3. Survival time of antimatter in the Milky Way and the early Universe

We can gain information about the properties of the antimatter regions and in particular constrain the amount of *normal* matter within them by estimating the typical lifetime of anti-matter in our Galaxy. The lifetime depends on the relative velocity between matter and antimatter particles, as the annihilation cross section can be strongly enhanced at low-velocity. For our estimates, we will follow the parametrization suggested in Ref. [36] and split the cross section in three regimes; a high-energy regime where the cross section scales with the inverse of the velocity; a Sommerfeld enhanced-regime where the cross section scales with the inverse of the *square* of the velocity; a saturation limit once the cross section reaches the size of an atom.[7] In practice, we use

$$\langle\sigma_{p\bar{p}}v\rangle \simeq \begin{cases} 1.5\times10^{-15}\ \mathrm{cm^3/s} & T > 10^{10}\ \mathrm{K}, \\ 10^{-10}\left(\frac{\mathrm{K}}{T}\right)^{1/2}\ \mathrm{cm^3/s} & 10^{10}\ \mathrm{K} > T > 10^{4}\ \mathrm{K}, \\ 10^{-10}\ \mathrm{cm^3/s} & 10^{4}\ \mathrm{K} > T. \end{cases} \tag{10}$$

The survival rate depends on whether antimatter is in the form of cold clouds, where $T \sim \mathcal{O}(30)$ K, or in hot ionized clouds, where $T \sim \mathcal{O}(10^6)$ K. In the former scenario, the lifetime $\tau_{\mathrm{ann}}^{\mathrm{cold}}$ is roughly

$$\tau_{\mathrm{ann}}^{\mathrm{cold}} = (n_p\langle\sigma_{p\bar{p}}v\rangle)^{-1} \simeq 10^{10}\left(\frac{n_p}{1\ \mathrm{cm^{-3}}}\right)^{-1}\ \mathrm{s}, \tag{11}$$

which is to be compared with the (much longer) age of our Galaxy $t_{\mathrm{gal}} \simeq 2.8\times10^{17}$ s. Hence, this requires the hydrogen density within cold antimatter clouds to verify

$$n_p^{\mathrm{cold}} < 3.5\times10^{-8}\ \mathrm{cm^{-3}}, \tag{12}$$

for such anticlouds to survive in our Galaxy. The same calculation in hot ionized cloud yields

$$\tau_{\mathrm{ann}}^{\mathrm{hot}} \simeq 1.7\times10^{13}\left(\frac{n_p}{1\ \mathrm{cm^{-3}}}\right)^{-1}\ \mathrm{s} \Rightarrow n_p^{\mathrm{hot}} < 6.1\times10^{-5}\ \mathrm{cm^{-3}}. \tag{13}$$

Note that these numbers are independent of the size and density of antimatter regions and agrees well with Refs. [36,38]. We conclude from this short analysis that antimatter would survive in our Galaxy only if there is some separation between the species, in which case it could be a viable candidate to explain the antihelium events. However, diffuse antimatter occupying all the volume of our Galaxy would not survive over the lifespan of our Galaxy.

Additionally, we can perform the same calculation in the early Universe, splitting between three periods depending on the annihilation regime. Before BBN, annihilations happen in the relativistic regime, and we can deduce

$$\tau_{\mathrm{ann}}(z > z_{\mathrm{BBN}}) \simeq \frac{3.3\times10^{21}}{(1+z)^3}\frac{n_p^{\mathrm{cosmo}}(z)}{n_p^{\mathrm{local}}(z)}\ \mathrm{s},$$

where $n_p^{\mathrm{local}}(z)$ and $n_p^{\mathrm{cosmo}}(z)$ respectively stand for the local and cosmological proton densities at redshift z while $z_{\mathrm{BBN}} \simeq 3.5\times10^9$. Comparing to the Hubble time at that epoch $t_H \simeq 5\times10^{19}(1+z)^{-2}$ s, we find that the hydrogen density inside antimatter regions must satisfy

$$\frac{n_p^{\mathrm{local}}}{n_p^{\mathrm{cosmo}}}(z > z_{\mathrm{BBN}}) < \left(\frac{67}{1+z}\right), \tag{14}$$

which means that, in the most optimistic scenario where such regions were formed right before BBN, the local proton density satisfies $n_p^{\mathrm{local}} < 1.9\times10^{-8}n_p^{\mathrm{cosmo}}$. After BBN, and roughly until matter-radiation equality, the constraint becomes

$$\tau_{\mathrm{ann}}(z_{\mathrm{eq}} < z < z_{\mathrm{BBN}}) \simeq \frac{8.3\times10^{16}}{(1+z)^{5/2}}\frac{n_p^{\mathrm{cosmo}}(z)}{n_p^{\mathrm{local}}(z)}\ \mathrm{s} \Rightarrow \frac{n_p^{\mathrm{local}}}{n_p^{\mathrm{cosmo}}}(z_{\mathrm{eq}} < z < z_{\mathrm{BBN}}) < \left(\frac{1.7\times10^{-3}}{\sqrt{1+z}}\right). \tag{15}$$

Finally, deep in the matter-dominated regime when antimatter is nonrelativistic and $t_H \simeq 8\times10^{17}(1+z)^{-3/2}$ we get

$$\tau_{\mathrm{ann}}(z < z_{\mathrm{eq}}) \simeq \frac{5\times10^{16}}{(1+z)^3}\frac{n_p^{\mathrm{cosmo}}(z)}{n_p^{\mathrm{local}}(z)}\ \mathrm{s} \Rightarrow \frac{n_p^{\mathrm{local}}}{n_p^{\mathrm{cosmo}}}(z < z_{\mathrm{eq}}) < \frac{6.3\times10^{-2}}{(1+z)^{3/2}}. \tag{16}$$

This confirms that antimatter must have formed in regions where the density of protons was much lower than the cosmological average (at least $\mathcal{O}(10^{-8})$ if these regions form just at the start BBN), such that annihilations only occur at the border of the antimatter dominated domains.

[7] We note that this parameterization has a discontinuity around 10^4 K, therefore the constraints obtained around that energy should be taken with a grain of salt. Fortunately, most of the constraining power comes from the regime where the cross section is well behaved.

It is conceivable that today these regions have survived in their pristine form, i.e., with little annihilation taking place inside them, although galaxy formation will likely have mixed up partially the species. Hence, this would imply the existence of some exotic segregation mechanism which makes the existence of such anticlouds rather improbable.

4. Constraints from the CMB

For over a decade, observations of the CMB have been used to constrain scenarios leading to exotic energy injection, in particular dark matter annihilations [60–80]. Interestingly, it is possible to recast constraints from these analyses onto the case of antimatter annihilations.[8] Since constraints on DM annihilation assume that the DM in our Universe is homogeneously distributed, they are only strictly applicable for the case of well mixed matter and antimatter regions. A full analysis of the case where energy is injected in an inhomogeneous manner is left to future work. To translate CMB bounds, we start by writing the energy injection rate from DM annihilation:

$$\left.\frac{\mathrm{d}^2E}{\mathrm{d}V\mathrm{d}t}\right|_{\mathrm{DM}} = \kappa\rho_c^2c^2\Omega_{\mathrm{CDM}}^2(1+z)^6\frac{\langle\sigma_{\mathrm{ann}}v\rangle}{m_{\mathrm{DM}}}. \tag{17}$$

where $\kappa = 1$ for Majorana particles and $\kappa = 1/2$ for Dirac particles. The DM density today is well known from CMB data and the prefactor $\rho_c^2c^2\Omega_{\mathrm{CDM}}^2 \simeq 4.5\times10^{-37}\ \mathrm{kg^2\,s^{-2}\,m^{-4}}$. In CMB analyses that constrain DM annihilation, the parameter $p_{\mathrm{ann}} \equiv \langle\sigma_{\mathrm{ann}}v\rangle/m_{\mathrm{DM}}$ is often introduced. Recently, the *Planck* collaboration has derived [82] $p_{\mathrm{ann}} < 1.8\times10^6\ \mathrm{m^3\,s^{-1}\,kg^{-1}}$, assuming a constant thermally averaged annihilation cross section times velocity (hereafter dubbed "the cross section" for simplicity).[9] Under this hypothesis, we can thus constrain the amount of energy injection from annihilation to be

$$\left.\frac{\mathrm{d}^2E}{\mathrm{d}V\mathrm{d}t}\right|_{\mathrm{ann}} < 8.1\times10^{-31}(1+z)^6\ \mathrm{J\,m^{-3}\,s^{-1}}. \tag{18}$$

This can be applied to the specific case of nonrelativistic antimatter annihilation

$$\left.\frac{\mathrm{d}^2E}{\mathrm{d}V\mathrm{d}t}\right|_{b\bar{b}\text{–ann}} = \langle\sigma_{p\bar{p}}v\rangle n_p n_{\bar{p}} 2m_pc^2 \tag{19}$$

leading to

$$n_{\bar{p}}^0 n_p^0 \lesssim 2.7\times10^{-5}\left(\frac{10^{-16}\ \mathrm{m^3/s}}{\langle\sigma_{p\bar{p}}v\rangle}\right)\ \mathrm{m^{-6}}. \tag{20}$$

Hence, we find $n_{\bar{p}}^0 < 1.35\times10^{-10}\ \mathrm{cm^{-3}}$ on cosmological scales, which is not in tension with *AMS-02* requirement (although strictly speaking the latter is valid within our Galaxy), as given by Eq. (8). We stress that the constraint derived here is very rough as CMB analyses rely on hypothesis of homogeneity and constant cross section, and thus deserves a thorough investigation in a separate paper if AMS measurement was confirmed.

5. Using gamma ray observations to place limits

Alternatively to searches using early Universe cosmology, gamma ray observations are routinely used to place constraints on exotic physics including dark matter annihilation or decay. There are three types of searches that have provided strong constraints on these scenarios: (i) searches for distinctive spectral features as would be the case for a gamma-ray line [85–88]; (ii) searches for morphological features localized on the sky, either from extended sources or from point sources on the sky (i.e., of angular size smaller than the point spread function of the instrument) [89–95]; (iii) searches for a continuous spectrum of gamma-rays extending over a large area on the sky as for instance from the extragalactic gamma-ray background [96–98]. In the following we present limits for the cases (i) and (ii) as they provide the strongest constraints on antimatter regions. Additionally, let us mention that, while we focus on annihilations of antiprotons, the requirement of overall neutrality of antiregions implies that there are as many positrons whose annihilations can also be searched for. For instance, in the case of annihilations (almost) at rest, we expect photons in the MeV range, extending down to the 511 keV line. These can be looked for in *INTEGRAL* data and will also lead to strong constraints on the presence of anti-clouds, a task we leave to future work.

Annihilations at rest and γ-ray line limit at 0.93 GeV We start by discussing constraints of type (i), which arise from nonrelativistic protons annihilating within or on the borders of the antimatter clouds/regions and resulting in gamma-rays. These gamma-rays will come from the channels that produce a neutral meson and a gamma-ray, as would be the case for $p\bar{p} \to \pi^0\gamma$, $\eta\gamma$, $\omega\gamma$, $\eta'\gamma$, $\phi\gamma$, $\gamma\gamma$. All these channels produce lines in the rest frame of the $p\bar{p}$-pair with energies between 0.66 and 0.938 GeV. The dominant reaction is the $\pi^0\gamma$ channel at 0.933 GeV with a branching ratio (BR) of 4.4×10^{-5}. Many more gamma-rays will come from the decays of neutral mesons produced from the $p\bar{p}$ annihilations, but these would result in a continuous spectrum below 0.938 GeV (see [99] for a full discussion on the $p\bar{p}$ annihilation products). A dedicated analysis accounting for all the annihilation channels would lead to stronger limits,

[8]The nonobservation of CMB spectral distortions can also be used to set constraints, but these are usually much weaker than that coming from anistropy power spectra analysis except if the cross section is boosted at high-velocities (e.g., p-wave) [81].

[9]Additionally, we assume here that all the energy is efficiently absorbed by the plasma for simplicity. This can overestimate the bound by up to an order of magnitude compared to more accurate analyses [64,71,83,84].

but is beyond the scope of this paper. However, there are limits from the Fermi-LAT observations on gamma-ray line features at these energies [88] which we use as a "proof-of-principle" that these studies can already severely constrain anticlouds. We make use of the constraints derived from the "R180" region [88] that covers the entire sky apart from a thin stripe along most of the Galactic plane and thus probes the averaged annihilation rate in a large part of the Milky Way around our location. Since most of the disk is excluded from the analysis, these constraints are to be taken with a grain of salt: it is conceivable that there are only a few highly dense clouds in our Galaxy contributing to the *AMS-02* flux, which would escape the analysis in Ref. [88]. Assuming on the other hand that antiregions are rather numerous and homogenously distributed in the Galactic disk, these constraints would be on the conservative side. We use the 95% upper limit flux of $\Phi_{\gamma\gamma}^{0.947} = 6.8 \times 10^{-7} \#\gamma\ \mathrm{cm}^{-2}\,\mathrm{s}^{-1}$, where $\Phi_{\gamma\gamma}$ just refers to the emission of two gamma-rays per annihilation event within an energy bin centered at 0.947 GeV and having a width of $\simeq$0.03 GeV.

Assuming antimatter to form cold clouds, we estimate the γ-production per unit volume to be

$$\begin{aligned}\rho_{\pi^0\gamma}^{\mathrm{MW}} &= \mathrm{Br}_{\pi^0\gamma}\left(\frac{V_{\overline{\mathrm{M}}} n_{\bar{p}}}{V_{\mathrm{M}}}\right) n_p \langle \sigma_{p\bar{p}} v\rangle \\ &\simeq 4.4\times 10^{-15}(10^{-5}\text{–}10^{-3.5})\left(\frac{n_b}{1\ \mathrm{cm}^{-3}}\right) \\ &\quad\times \left(\frac{n_p^{\mathrm{local}}}{1\ \mathrm{cm}^{-3}}\right) \#\gamma\ \mathrm{cm}^{-3}\,\mathrm{s}^{-1}, \end{aligned} \tag{21}$$

where the ratio $V_{\overline{\mathrm{M}}} n_{\bar{p}}/V_{\mathrm{M}}$ is given by Eq. (8) and we make the distinction between the average baryon number density in the Galaxy n_b and the density of proton within anticlouds n_p^{local}. We assume that this rate is homogeneous in the Galactic disk (as would arise from a scenario with numerous clouds) but drops as we move perpendicularly away from the Galactic plane, following a Gaussian[10] with a width σ_z of 0.1 kpc. Integrating along the line of sight and averaging over all relevant directions for R180 of [88], the gamma-ray line flux is

$$\begin{aligned}\Phi_{\pi^0\gamma}^{m_p} &= \frac{\int^{R180} d\ell\, d\Omega \rho_{\pi^0\gamma}^{\mathrm{MW}}}{\int^{R180} d\Omega} \\ &= 2.42\times(10^2\text{–}10^{3.5})\left(\frac{n_b}{1\ \mathrm{cm}^{-3}}\right)\left(\frac{n_p^{\mathrm{local}}}{1\ \mathrm{cm}^{-3}}\right)\#\gamma\,\mathrm{cm}^{-2}\,\mathrm{s}^{-1}. \end{aligned} \tag{22}$$

This is a factor of 4.4×10^8–1.1×10^{10} larger than the reported limit (we recall that the uncertainty range comes from the uncertainty on $\bar{\eta}$). We point out that while this result is an approximation that relies on certain assumptions on the anti-matter distribution properties, as well as on the level of overlap of matter and antimatter, such a strong tension cannot be easily circumvented. In fact we consider these limits to be very constraining of such a possibility unless matter and antimatter regions overlap only by $\mathcal{O}(10^{-10})$, such that the density of matter within antiregion is constrained to be

$$n_p^{\mathrm{local}} \lesssim 10^{-10} - 2\times 10^{-9}\ \mathrm{cm}^{-3}. \tag{23}$$

In the case of hot clouds, note that this constraint can relax by a factor of $\mathcal{O}(2000)$. We recall that those limits are calculated based on an optimization of the region of interest ("R180" in this case) that was chosen for a possible signal of DM decay all over the DM halo, and in fact are not optimal for searching a gamma-ray line signal from ambient antimatter or antimatter clouds in the Galactic disk. They would apply—and are conservative—if anticlouds are numerous and distributed following the Galactic disk profile, while they vanish if there are only a few very dense anticlouds in our Galaxy.

γ-rays from CR annihilations in close-by anti-clouds Even though anticlouds are devoid of matter so that the above mentioned constraints are satisfied, nothing prevents CR protons to penetrate into these clouds where they annihilate. Contrary to a spectral feature arising from annihilation at rest, accelerated particles such as CR can yield a strong annihilation signal appearing as a continuous emission. Moreover, localized features on the sky (case ii) in previous discussion) can arise if antimatter regions are well localized in space. Of the *regular* matter clouds, the densest are the molecular clouds that have sizes from tenths of a parsec up to $\mathcal{O}(10)$ pc, with the smallest ones in size having number densities as high as $10^6\ \mathrm{cm}^{-3}$ [100]. Instead the cold and warm atomic Hydrogen is more diffuse but large clouds can have sizes of $\sim$100 pc with densities of 0.2–50 cm^{-3} [100]. Finally ionized gas clouds have densities of 7×10^{-3}–0.5 cm^{-3} with a maximum size of $\mathcal{O}(100)$ pc.

As we have discussed previously, *AMS-02* does not give a precise measurement of the density of antimatter, but rather constrains the product of the total volume and density of these regions [see Eq. (8)]. To avoid making exact assumptions on the size and density of these clouds (since these two parameters vary observationally by many orders of magnitude) we will assume that antimatter clouds have a typical mass of $M_{\bar{c}} \equiv V_{\bar{c}} m_{\bar{b}} n_{\bar{b}} = 10^3\ M_\odot$.[11] In that case there are,

[10]This choice is arbitrary and just ensures that the gas and antigas density drops abruptly above and below the Galactic plane. We checked that using a more sharply dropping hyperbolic tangent gives similar result.

[11]From observations on matter clouds that quantity can also vary by at least a couple of orders of magnitude either toward larger or smaller mass values.

$$N_{\bar{c}} = \frac{V_M n_b m_p}{M_{\bar{c}}}(10^{-5}\text{–}10^{-3.5}) \simeq 1.6\times 10^4(10^{-1.5}\text{–}1)\left(\frac{M_b^{\rm MW}}{5\times 10^{10}\ M_\odot}\right)\left(\frac{M_{\bar{c}}}{10^3\ M_\odot}\right)^{-1}, \quad (24)$$

where $M_b^{\rm MW}$ is the total mass of baryons in the Milky Way and where, as usual, we made use of Eq. (8). We can estimate the typical distance $D_{\bar{c}}$ separating these objects (and therefore the Earth from them), assuming that within the Galactic disk the antimatter clouds are homogeneously distributed. We get

$$D_{\bar{c}} \simeq \frac{1}{2}\left(\frac{V_M}{N_{\bar{c}}}\right)^{1/3} \simeq 80\ {\rm pc}\times(1\text{–}10^{0.5})\left(\frac{V_M}{6\times 10^{10}\ {\rm pc}^3}\right)^{1/3} \times\left(\frac{M_b^{\rm MW}}{5\times 10^{10}\ M_\odot}\right)^{-1/3}\left(\frac{M_{\bar{c}}}{10^3\ M_\odot}\right)^{1/3}. \quad (25)$$

If such a cloud is of a size < 1 pc its angular extension is $\simeq 0.7°$. Hence, even the closest antimatter cloud would appear as a point source at gamma-ray energies of 1 GeV. The local CR proton spectrum is $dN/dE \simeq 10^3(E/1\ {\rm GeV})^{-2.8}\ {\rm m^{-2}\,s^{-1}\,sr^{-1}\,GeV^{-1}}$ [101]. These protons colliding with antiprotons would give relativistic neutral mesons that after decaying would result in a similar gamma-ray spectrum above ~1 GeV. At gamma-ray energies between 1–3 GeV the flux is,

$$\Phi_\gamma = \frac{L_\gamma}{4\pi D_{\bar{c}}^2} = \frac{1}{4\pi D_{\bar{c}}^2}\int dV_{\bar{c}} n_{\bar{p}} n_p \sigma_{p\bar{p}} v = 1.2\times 10^{-9}(10^{-1}\text{–}1)\left(\frac{V_M}{6\times 10^{10}\ {\rm pc}^3}\right)^{-2/3} \times\left(\frac{M_b^{\rm MW}}{5\times 10^{10}\ M_\odot}\right)^{2/3}\left(\frac{M_{\bar{c}}}{10^3\ M_\odot}\right)^{1/3} \#\gamma\ {\rm cm^{-2}\,s^{-1}}. \quad (26)$$

We have assumed here four photons per annihilation coming from the average π^0 multiplicity of $\simeq 2$ from $p\bar{p}$ annihilations [99]. We took the branching ratio to neutral mesons to be 4% and have integrated dN/dE between 3 and 10 GeV for the CR protons, in order to be able to directly compare to the Fermi-LAT point source sensitivity at the same energy range as reported in Ref. [102]. Note that at such energies, we can use the high-energy limit of Eq. (10) for the annihilation cross section. For this energy range the sensitivity is $\Phi_\gamma \simeq 10^{-10}\#\gamma\ {\rm cm^{-2}\,s^{-1}}$. Using Eq. (26), we deduce that such annihilations would be detectable up to a distance of 0.1–0.3 kpc. From Eq. (25), we conclude that roughly 2–40 point sources could be detectable. Interestingly, a number of these could contribute to the 334 3FGL unassociated point sources in the Galactic plane[12] (within Galactic latitude $|b| < 5°$). Alternatively, the nondetection of anticlouds by the Fermi LAT allows to constrain the number (and in turn the mass) of these objects. Note that this constraint does not depend on the amount of matter within antimatter domains; as CR propagate they would travel through antiregions even if these are poor in matter originally. Hence, this estimate is fairly robust to conditions occurring within antidomains. Also, a careful analysis of the spectrum of the unassociated sources would be necessary to assess whether these are anticloud regions. For instance, we anticipate that when annihilations between antiprotons and protons occur nearly at rest (as is in most cases), then a continuous spectrum in gamma-rays with a cutoff at $\simeq 1$ GeV should always be produced. A proper population analysis should also take into account the variation in the luminosity of these new type of sources depending on their size and their distance from the Earth.

Finally, we point out that one could also do a dedicated search for extended continuous spectrum features on the Galactic sky; i.e., what we described as type (iii). These could be coming from very close-by anticloud regions or from the combined emission of a very large number of them along the Galactic-disk plane. Given the uncertainties on their distribution and that one would also need to account for the many charged pions produced by the $p\bar{p}$ annihilations leading to $e^\pm$ pairs which in turn if relativistic would give inverse Compton scattering as they propagate though the Milky-Way, this possible search channel is beyond the scope of this paper. At low-energies, we know from *INTEGRAL* observations that $e^\pm$ pairs pervade the inner parts of the Galaxy [103–105]. From *Fermi*-LAT studies, we also know of the GeV Galactic Center excess in gamma-rays [106–111]. Yet, neither the Galactic center excess, nor the 511-keV line are strongly correlated to known gas structures. Moreover, the Galactic center excess has a high-energy tail that would demand highly boosted antimatter that has survived in a dense matter environment. In conclusion, we consider it very unlikely that these excesses could be associated to anticloud regions.

6. Using cosmic ray antimatter observations to look for antiregions

One of the important questions associated to anticlouds is the acceleration of antimatter within the cloud. Supernovae shock waves, following the explosion of a massive star,[13] accelerate the material in the ISM. Any

[12]We note that over the entire sky, there are 992 unidentified point sources.

[13]This acceleration mechanism could also arise from the explosion of a massive antistar, if such regions with that massive stars still exist.

antimatter particle within—or close to—these environments can also be accelerated by these waves. The spectra of the injected particles would be very similar to that of normal matter, i.e., following a power law in energy with index ∼2.2–2.8. The index values of ≃2.7–2.8 come naturally for CR protons and He at ∼10–200 GeV, as a result of several SNRs in the Milky-Way, i.e., the averaged CR nuclei spectra. A harder index value of 2.4 or 2.2 would instead arise if a near-by (of ∼kpc or ∼100 pc distance) SNR was the dominant contributor of CR antiparticles observed by *AMS-02*.

Interestingly, from our BBN range of $\bar{\eta}$-values (and given the uncertainties on the injection index of these CRs) we can calculate what fluxes of $\bar{p}$ and $\bar{d}$ should be expected in *AMS-02* data. Antiproton data from *AMS-02* are already available and can alternatively be used to place constraints on the $\bar{p}$ primary CR flux component (coming from the acceleration of the ISM $\bar{p}$).

We calculate first the $\bar{p}$ flux from the primary component associated with the $\overline{^3\mathrm{He}}$ and $\overline{^4\mathrm{He}}$ events. We evaluate first 3–σ upper limits from the $\bar{p}/p$ ratio [112]. To set the normalization, we take into account that eight $\overline{^3\mathrm{He}}$ and $\overline{^4\mathrm{He}}$ events have been observed with at least one with $E_{\rm kin}/n$ between 6 and 10 GeV. Moreover, we account for all the relevant uncertainties. These are associated with,

(i) The injection and propagation through the ISM of the matter CRs, mainly protons and Helium nuclei, that through the inelastic collisions with the ISM gas lead to the production of the conventional secondary $\bar{p}$s. The part of the ISM uncertainties affects also the propagation of the secondary $\bar{p}$s.
(ii) The antiproton production cross section from these collisions, affecting the spectrum and overall flux of the secondary $\bar{p}$ component.
(iii) The matter gas in the local ISM affecting the overall normalization of the secondary $\bar{p}$ component.
(iv) The Solar modulation of CRs as they propagate through the Heliosphere before getting detected by *AMS-02*. These uncertainties affect both the secondary and primary $\bar{p}$ components as well as the heavier anti-nuclei fluxes.
(v) The primary $\bar{p}$ flux index n range of 2.2–2.8 that is associated with the uncertainties of their propagation through the ISM, i.e., their locality of origin or not.
(vi) The $\bar{\eta}$-range of $1.3–6 \times 10^{-13}$, affecting the ratios of primary antinuclei fluxes.

To account for the first four of the above mentioned uncertainties we marginalize over them following the prescription of Ref. [113] based on results of Refs. [42,114]. For the latter two we just take a few extreme cases of $(n, \bar{\eta}) = (2.2, 1.3 \times 10^{-13})$, $(2.4, 1.3 \times 10^{-13})$ $(2.8, 1.3 \times 10^{-13})$, $(2.2, 6 \times 10^{-13})$, $(2.4, 6 \times 10^{-13})$ and $(2.8, 6 \times 10^{-13})$. The primary $\bar{p}$ flux are described by,

$$\frac{dN^{\bar{p}}}{dE_{\rm kin}} = \mathrm{Norm}^{\bar{p}} \left(\frac{E_{\rm kin}}{1\ \mathrm{GeV}}\right)^{-n} (\mathrm{GeV}^{-1}\,\mathrm{m}^{-2}\,\mathrm{s}^{-1}\,\mathrm{sr}^{-1}), \quad (27)$$

and in turn the $\bar{d}$ and $\overline{\mathrm{He}}$ (: $\overline{^3\mathrm{He}}$ & $\overline{^4\mathrm{He}}$) primary fluxes are,

$$\frac{dN^{\bar{d}}}{dE_{\rm kin}} = \frac{\bar{d}}{\bar{p}}(\bar{\eta}) \frac{dN^{\bar{p}}}{dE_{\rm kin}} \quad \text{and} \quad (28)$$

$$\frac{dN^{\overline{\mathrm{He}}}}{dE_{\rm kin}} = \frac{\overline{\mathrm{He}}}{\bar{p}}(\bar{\eta}) \frac{dN^{\bar{p}}}{dE_{\rm kin}}, \quad (29)$$

where $E_{\rm kin}$ is the per nucleon kinetic energy. For $\bar{\eta} = 1.3 \times 10^{-13}$, $\bar{d}/\bar{p} \simeq 10^{-2.5}$, $\overline{\mathrm{He}}/\bar{p} \simeq 10^{-5.5}$, while for $\bar{\eta} = 6 \times 10^{-13}$, $\bar{d}/\bar{p} \simeq 10^{-2}$, $\overline{\mathrm{He}}/\bar{p} \simeq 10^{-4}$.

In general, we find that anti-clouds can leave significant traces in the $\bar{p}/p$ ratio. In fact, depending on the propagation configuration, it could even lead to an excess of antiprotons. For instance, for an injection index of $n = 2.2(2.4)$ and a given propagation model (model E of Ref. [114]), we find that the $\bar{p}/p$ ratio of *AMS-02* [112] can restrict $\bar{\eta} \geq 1.3(2.0) \times 10^{-13}$ at 3–σ (the proportion of $\bar{p}$ decreases as $\bar{\eta}$ increases). If we saturate this limit, we predict $5.1(2.7) \times 10^4$ primary CR $\bar{p}$ detected events by *AMS-02* after 6 years of data collection and $0.1 < \bar{d}$ events in the same period. If instead we assume $n = 2.8$, we find that $\bar{\eta} \geq 4 \times 10^{-13}$, and predict 8.4×10^3 primary CR $\bar{p}$ in *AMS-02* data and again only ≃0.1 $\bar{d}$s.

In conclusion, CRs provide a strong probe of the anticloud scenarios. Interestingly, a number of $\bar{p}$ events detected by *AMS-02* might originate from antiregions. The *GAPS* experiment, sensitive to $\bar{d}$ at lower energies than *AMS-02*, could detect a few events. A study of the implication of this finding in light of the recent claims of an excess of antiprotons at ten's of GeV energies [27] would be worthwhile.

B. Antistars in a dense environment

1. Properties of antistars from AMS-02 measurement

An alternative possibility is that the antimatter is in the form of stars. This is likely more realistic, since antistars would naturally be free of matter at their heart, and annihilation are limited to their surface. In that case, the isotopic ratio measured by *AMS-02* can inform us about the stellar population. Taken at face value, the presence of a high number of $\overline{^3\mathrm{He}}$ is also difficult to explain in this scenario. One possibility is that antistars are relatively light. Indeed, by analogy with normal matter, the main material within an antistar with $M_* \lesssim 0.6\ M_\odot$ (but higher than $0.08\ M\odot$ such as to initiate hydrogen fusion into deuterium) could be $\overline{^3\mathrm{He}}$. This would however require the presence of low density regions so that the primordial material from which the star has formed is poor in

antihelium-4, and this scenario is thus affected by the same difficulty as the anticloud one.

A more realistic case, already suggested in Ref. [115], and more recently in Ref. [116] is that the antistar has formed from a very dense clump within an antimatter domain, which could have survived since the early Universe. BBN in a very dense medium would result in the creation of very large amounts of $\overline{^4\mathrm{He}}$, so that the antistar could be largely dominated by $\overline{^4\mathrm{He}}$. Difficulties associated to this scenario are two fold: (i) a mechanism responsible for the acceleration of $\overline{^4\mathrm{He}}$ up to 50 GeV energy is required; (ii) the isotopic ratio $\overline{^4\mathrm{He}}:\overline{^3\mathrm{He}}$ must be inverted during propagation close to the source.

Depending on the answer to point (i), the estimate of the number of such objects can largely vary. A single close-by antistar might be responsible for the entire antihelium flux seen by *AMS-02*. A possible acceleration mechanism is that large chunks of normal matter, e.g., asteroid-mass clumps, hit the antistar, resulting in a powerful annihilation reaction which would eject and accelerate $\overline{^4\mathrm{He}}$ nuclei from within the antistar. Impacts of asteroid-mass clumps with neutron stars are, for example, key elements of a current model for fast radio bursts as in Ref. [117] and have been used to constrain the possible presence of antimatter in our Galaxy [96]. As a more relevant example, we estimate that an object of the size of the Earth annihilating onto the surface of such an antistar could liberate an energy of order $\sim 10^{49}$ ergs. This is enough for a shell of antimatter with mass $\sim 0.01\ \mathrm{M}_\odot$ to be expelled in outer space with a velocity of 10^4 km/s. This coincides with half the rotational energy of the Crab pulsar which is a well-known potential source of high-energy positrons and electrons. To quantify, if a fraction $f_{\rm acc}$ of a *single* antistar experienced such an event, the total amount of antihelium ejected in the Galaxy would be approximately

$$\begin{aligned}\Phi_{\overline{\rm He}} &= \left(\frac{c}{V_{\rm gal}}\right)\left(\frac{f_{\overline{\rm He}} M_{\bar{*}}}{m_{\overline{\rm He}}}\right) f_{\rm acc} \\ &\simeq 10^{-9}\left(\frac{(4\pi/3)(10\ \mathrm{kpc})^3}{V_{\rm gal}}\right)\left(\frac{M_{\bar{*}}}{M_\odot}\right) \\ &\quad\times\left(\frac{f_{\rm acc}}{10^{-8}}\right)\left(\frac{f_{\overline{\rm He}}}{1}\right)\#\overline{\rm He}\ \mathrm{cm^{-2}\,s^{-1}}, \end{aligned} \tag{30}$$

where $f_{\overline{\rm He}}$ represents the fraction of antihelium-4 within the antistar. Interestingly, for $f_{\overline{\rm He}} = 1$ and $f_{\rm acc} = 10^{-8}$, this is in good agreement with the measured *AMS-02* flux in the GeV range. However, given that CR nuclei stay confined within the magnetic halo over a timescale ranging from $\sim 10^7$ to 3×10^8 yr, which is short compared to the $\sim 10^{10}$ yr of existence of our Galaxy, the probability that such an event occurred nowadays is smaller than 3%, and it is therefore more likely that there exists a population of such stars. If antistars are formed in star clusters, more conventional acceleration mechanisms (e.g., SN shock-waves, jets, outflows) can also be responsible for CRs antihelium at such energies. We note that massive stars leading to SN explosions are short-lived, and therefore primordial antistars would most likely not survive over the course of the Universe. This acceleration mechanism would require to form antistars from the gas at a much later time. Given the strong constraints on the anticlouds scenario, this case seems disfavored. However, one of these other routes to antimatter CR acceleration from antistars is the case where a binary of antimatter white dwarfs would merge giving an antimatter type Ia supernova. Regular white-dwarf mergers occur at a rate per unit stellar mass of $1.4 \times 10^{-13}\ \mathrm{yr^{-1}\,M_\odot^{-1}}$ [118]. Requiring that at least one binary of antimatter white dwarfs merges over a typical CR diffusion timescale translates into a minimal stellar population of antistars of $\sim 2.4 \times 10^4$ to $7 \times 10^5\ \mathrm{M}_\odot$ within 10 kpc from the Earth. This is very small compared to the Galactic stellar population which amounts to $\sim 6 \times 10^{10}\ \mathrm{M}_\odot$. In order to achieve point (ii), spallation around the source needs to be efficient enough such as to convert a large amount of $\overline{^4\mathrm{He}}$ into $\overline{^3\mathrm{He}}$. Given the total cross section for $\bar{p}^4\mathrm{He}$ interactions as well as the fraction of events going into $^3\mathrm{He} + X$ measured by the Lear collaboration [119], we estimate that a grammage of order $20\ \mathrm{g/cm^2}$ would be enough to generate an isotopic ratio $\overline{^3\mathrm{He}}:\overline{^4\mathrm{He}}$ of roughly 3:1. A similar estimate can be calculated from the measurement of the isotopic ratio of $^4\mathrm{He}:^3\mathrm{He}$ by *PAMELA* [56], that is ∼5:1 aroAund a few GeV/n, and from the fact that the grammage in our Galaxy below 100 GeV is $\sim 3\ \mathrm{g/cm^2}$ (deduced from B/C analysis [120]). The grammage required for antihelium is reasonable as it corresponds to a layer 200 m thick with density $10^{-3}\ \mathrm{g/cm^3}$, i.e., 1/50th of our atmosphere. If true, the origin of this grammage would most likely be related to the origin of the antistar itself. Indeed, we expect antistars to be surrounded by much denser material than that around normal stars, as the former are born from large over-densities at a much earlier time.

2. Constraints on antistars

Given that a single antistar could explain *AMS-02* data, there is no strong constrain on the presence of such objects in our Galaxy. Indeed, even if all of the antihelium-4 is converted to antiprotons, it would only lead to a handful of events that can easily be hidden within the $\sim 10^5$ $\bar{p}$ events observed by *AMS-02* [112]. We can however constrain the presence of such object in the vicinity of the Sun. Assuming spherical (Bondi) accretion and making use of unidentified source in the 2FGL Fermi-LAT catalog, Ref. [121] constrained the local environment, within 150 pc from the Sun, to have $N_{\bar{*}} < 4 \times 10^{-5} N_*$. The brightest unassociated source from the 3FGL catalog emits

$2 \times 10^{-8} \#\gamma\ \mathrm{cm}^{-2}\,\mathrm{s}^{-1}$ above 1 GeV [102]. From this, we can estimate the distance of the closest antistar assuming that its luminosity is sourced by annihilation at its surface. The luminosity associated to the emission is

$$L_{\bar{\star}} = 8\pi R_{\bar{\star}}^2 v n_p \simeq 10^{31} \left(\frac{R_{\bar{\star}}}{10^{11}\ \mathrm{cm}}\right)^2 \left(\frac{v}{300\ \mathrm{km\,s^{-1}}}\right) \left(\frac{n_p}{1\ \mathrm{cm^{-3}}}\right) \#\gamma\ \mathrm{s}^{-1}, \tag{31}$$

where we assumed that the dominant channel for prompt photon emission is through π_0 production (whose average multiplicity is 2 per annihilation at rest [99]). The minimal distance of such an object is obtained by requiring

$$\frac{L_{\bar{\star}}}{4\pi d_{\bar{\star}}^2} \leq 2 \times 10^{-8} \#\gamma\ \mathrm{cm}^{-2}\,\mathrm{s}^{-1}, \tag{32}$$

which yields

$$d_{\bar{\star}} \geq 6 \times 10^{18} \sqrt{\left(\frac{R_{\bar{\star}}}{10^{11}\ \mathrm{cm}}\right) \left(\frac{v}{300\ \mathrm{km\,s^{-1}}}\right) \left(\frac{n_p}{1\ \mathrm{cm^{-3}}}\right)}\ \mathrm{cm}. \tag{33}$$

Hence, it is possible that an antistar whose main source of emission is annihilation at its surface lies in a close-by environment $\sim\mathcal{O}(1\ \mathrm{pc})$ away from the Sun.

Although constraints in our Galaxy are weak, bounds on the scenario can potentially be derived from annihilations and energy injection in the early Universe. Any realistic scenario would lead to the creation of a population of such objects that in turn could lead to spectral distortions of the CMB and modify the CMB anisotropy power spectra. We have calculated in Sec. III A 4 the specific case of homogeneously distributed antimatter domains. A similar calculation can be done to get a rough constraint on the number density of antistars from CMB data. We can calculate the energy injection rate from annihilation at the surface of an antistar moving in the photon-baryon plasma at a velocity $v \sim 30\ \mathrm{km/s}$ (the typical relative velocity between baryons and CDM-like component at early times [122]):

$$\left.\frac{\mathrm{d}^2 E}{\mathrm{d}V \mathrm{d}t}\right|_{\bar{\star}} = 8\pi R_{\bar{\star}}^2 v n_p m_p c^2 n_{\bar{\star}} \simeq 10^{13} n_{\bar{\star}}\ \mathrm{J\ s^{-1}} \times \left(\frac{R_{\bar{\star}}}{10^{11}\ \mathrm{cm}}\right) \left(\frac{v}{30\ \mathrm{km\,s^{-1}}}\right) \left(\frac{n_p^0}{2 \times 10^{-7}\ \mathrm{cm^{-3}}}\right). \tag{34}$$

Applying the constraints from *Planck* given by Eq. (18), we can derive that on cosmological scales

$$n_{\bar{\star}} \lesssim 10^{24} (1+z)^3\ \mathrm{Mpc}^{-3}, \tag{35}$$

which trivially satisfies AMS measurements. We stress that this very weak constraint assumes that the main source of ionizing radiation is annihilation at the surface of antistars. A more accurate constraint would also take into account radiation coming from nuclear processes at play within antistars, which would require additional assumptions about these objects.

IV. DISCUSSION AND CONCLUSIONS

In this work, we have studied the implications of the potential discovery of antihelium-3 and -4 nuclei by the *AMS-02* experiment. Using up-to-date semi-analytical tools, we have shown that it is impossible to explain these events as secondaries, i.e., from the spallation of CR protons and helium nuclei onto the ISM. The $\overline{^3\mathrm{He}}$ is typically one to two orders of magnitude below the sensitivity of *AMS-02* after 5 years, and the $\overline{^4\mathrm{He}}$ is roughly 5 orders of magnitude below *AMS-02* reach. It is conceivable that $\overline{^3\mathrm{He}}$ has been misidentified for $\overline{^4\mathrm{He}}$. Still, we have argued that the pure secondary explanation would require a large increase of the coalescence momentum at low energies, a behavior that goes against theoretical considerations and experimental results. The DM scenario suffers the same difficulties. Hence, we have discussed how this detection, if confirmed, would indicate the existence of an antiworld, in the form of antistars or anticlouds. We summarize what we have learned about the properties of antimatter regions:

(i) Taken at face value the isotopic ratio of antihelium nuclei is puzzling. We have shown that it can be explained by anisotropic BBN in regions where $\bar{\eta} \sim 1.3\text{–}6 \times 10^{-13}$.

(ii) The density, size and number of antimatter domains is constrained by *AMS-02* observations and our knowledge of Galactic properties to verify Eq. (9). The only theoretical assumption behind is that the isotopic ratio measured by *AMS-02* comes from BBN. Interestingly, a few highly dense clouds are sufficient to explain *AMS-02* measurements.

(iii) The annihilation rate of antimatter in our Galaxy requires antidomains to be poor in normal matter (typically a tenth or less of the normal matter density). Considering the annihilation rate in the early Universe leads to even stronger requirements, which would imply the existence of some exotic mechanism allowing segregation of matter and antimatter domains all along cosmic evolution that makes the existence of such anticlouds quite improbable.

(iv) Additionally, gamma rays can provide strong constraints on this scenario. Nonobservation of spectral features in the form of lines with energies close to

the proton mass strongly constrains the proton density in antimatter domain, as given by Eq. (23). However, this constraints apply only if antimatter domains are numerous and homogeneously distributed within the Galactic disk. We anticipate that very competitive constraints can be obtained from nonobservation of positron annihilations and/or pion decays.

(v) Anticlouds could produce a measurable flux of $\bar{p}$ and $\bar{d}$. Most of the parameter space evades current $\bar{p}$ constraints but could be probed by GAPS.

(vi) Alternatively (and more likely), these antihelium events could originate from antistar(s) whose main material is antihelium-4, converted into antihelium-3 via spallation in the dense environment surrounding the antistar(s).

(vii) Part of the 3FGL unassociated point sources can be anticlouds experiencing annihilations due to CRs propagating through them. They can also be antistars which experience annihilations as they propagate in the ISM.

(viii) Depending on the (unknown) acceleration mechanism, it is conceivable that a single near-by antistar (whose distance to the Earth must be larger than $\sim$1 pc) contributes to the *AMS-02* observation.

All these hints can be used to build a scenario for their formation in the early Universe. Needless to say, the successful creation and survival of such objects within a coherent cosmological model is far from obvious. Here we just mention that there are many scenarios discussed in the literature [38,116,123], including the Affleck-Dine mechanism [124], which would lead to the formation of "bubbles" of matter and antimatter with arbitrarily large values of the baryon-asymmetry locally. Depending on the relation between their mass and the corresponding Jeans mass, these bubbles can then lead to the formation of antistarlike objects, either through specific inflation scenarios with large density contrast [125,126] on scales reentering the horizon around the QCD phase-transition, i.e., $T \sim \mathcal{O}(100\ \mathrm{MeV})$, or from peculiar dynamics of the plasma within the bubble, as described for instance in Ref. [115]. In the latter scenario, the *negative* pressure perturbation inside the bubble leads to the collapse of baryons within this region. If the value of the baryon-asymmetry in the bubble is very large, it is even possible that different expansion rate (due to more nonrelativistic matter inside the bubble) naturally leads to the growth of density perturbations much earlier than outside of these regions. Given the strong implications of the discovery of a single antihelium-4 nucleus for cosmology, important theoretical and experimental efforts must be undertaken in order to assess whether the reported events could be explained by a more mundane source, such as interactions within the detector, or another source of yet unknown systematic error. Still, this potential discovery would represent an important probe of conditions prevailing in the very early Universe and should be investigated further in future work.

ACKNOWLEDGMENTS

We thank Kim Boddy, Kfir Blum and Robert K. Schaefer for very interesting discussions. We thank Annika Reinert and Martin Winkler for clarifications about the antiproton cross section parametrization. We thank Alexandre Arbey for his help with the AlterBBN code, as well as Elisabeth Vangioni, Alain Coc, Cyril Pitrou and Jean-Philippe Uzan for helping us check our results with the PRIMAT code. We thank Pasquale D. Serpico, Philip von Doetinchem and Julien Lavalle for their critical and insightful comments on an earlier version of this draft. This work was partly supported at Johns Hopkins by NSF Grant No. 0244990, NASA NNX17AK38G, and the Simons Foundation. P. S. would like to thank Institut Universitaire de France for its support. This research project was conducted using computational resources at the Maryland Advanced Research Computing Center (MARCC).

[1] O. Adriani *et al.* (PAMELA Collaboration), Phys. Rev. Lett. **105**, 121101 (2010).
[2] L. Bergstrom, T. Bringmann, and J. Edsjo, Phys. Rev. D **78**, 103520 (2008).
[3] M. Cirelli and A. Strumia, Proc. Sci., IDM2008 (**2008**) 089.
[4] M. Cirelli, M. Kadastik, M. Raidal, and A. Strumia, Nucl. Phys. **B813**, 1 (2009); **B873**, 530(A) (2013).
[5] A. E. Nelson and C. Spitzer, J. High Energy Phys. 10 (2010) 066.
[6] N. Arkani-Hamed, D. P. Finkbeiner, T. R. Slatyer, and N. Weiner, Phys. Rev. D **79**, 015014 (2009).
[7] R. Harnik and G. D. Kribs, Phys. Rev. D **79**, 095007 (2009).
[8] P. J. Fox and E. Poppitz, Phys. Rev. D **79**, 083528 (2009).
[9] M. Pospelov and A. Ritz, Phys. Lett. B **671**, 391 (2009).
[10] J. D. March-Russell and S. M. West, Phys. Lett. B **676**, 133 (2009).
[11] K. R. Dienes, J. Kumar, and B. Thomas, Phys. Rev. D **88**, 103509 (2013).
[12] J. Kopp, Phys. Rev. D **88**, 076013 (2013).
[13] H. Yuksel, M. D. Kistler, and T. Stanev, Phys. Rev. Lett. **103**, 051101 (2009).
[14] S. Profumo, Central Eur. J. Phys. **10**, 1 (2011).

[15] N. Kawanaka, K. Ioka, and M. M. Nojiri, Astrophys. J. **710**, 958 (2010).
[16] Q. Yuan, X.-J. Bi, G.-M. Chen, Y.-Q. Guo, S.-J. Lin, and X. Zhang, Astropart. Phys. **60**, 1 (2015).
[17] P.-F. Yin, Z.-H. Yu, Q. Yuan, and X.-J. Bi, Phys. Rev. D **88**, 023001 (2013).
[18] D. Hooper, P. Blasi, and P. D. Serpico, J. Cosmol. Astropart. Phys. 01 (2009) 025.
[19] I. Cholis, D. P. Finkbeiner, L. Goodenough, and N. Weiner, J. Cosmol. Astropart. Phys. 12 (2009) 007.
[20] I. Cholis, L. Goodenough, D. Hooper, M. Simet, and N. Weiner, Phys. Rev. D **80**, 123511 (2009).
[21] I. Cholis and D. Hooper, Phys. Rev. D **88**, 023013 (2013).
[22] M. Boudaud *et al.*, Astron. Astrophys. **575**, A67 (2015).
[23] M. Boudaud, E. F. Bueno, S. Caroff, Y. Genolini, V. Poulin, V. Poireau, A. Putze, S. Rosier, P. Salati, and M. Vecchi, Astron. Astrophys. **605**, A17 (2017).
[24] D. Hooper, I. Cholis, T. Linden, and K. Fang, Phys. Rev. D **96**, 103013 (2017).
[25] I. Cholis, T. Karwal, and M. Kamionkowski, Phys. Rev. D **97**, 123011 (2018).
[26] I. Cholis, T. Karwal, and M. Kamionkowski, Phys. Rev. D **98**, 063008 (2018).
[27] A. Cuoco, M. Krmer, and M. Korsmeier, Phys. Rev. Lett. **118**, 191102 (2017).
[28] A. Reinert and M. W. Winkler, J. Cosmol. Astropart. Phys. 01 (2018) 055.
[29] P. Chardonnet, J. Orloff, and P. Salati, Phys. Lett. B **409**, 313 (1997).
[30] F. Donato, N. Fornengo, and P. Salati, Phys. Rev. D **62**, 043003 (2000).
[31] R. Duperray, B. Baret, D. Maurin, G. Boudoul, A. Barrau, L. Derome, K. Protasov, and M. Buenerd, Phys. Rev. D **71**, 083013 (2005).
[32] P. von Doetinchem *et al.*, Proc. Sci., ICRC2015 (**2016**) 1218.
[33] E. Carlson, A. Coogan, T. Linden, S. Profumo, A. Ibarra, and S. Wild, Phys. Rev. D **89**, 076005 (2014).
[34] M. Cirelli, N. Fornengo, M. Taoso, and A. Vittino, J. High Energy Phys. 08 (2014) 009.
[35] A. Coogan and S. Profumo, Phys. Rev. D **96**, 083020 (2017).
[36] G. Steigman, Annu. Rev. Astron. Astrophys. **14**, 339 (1976).
[37] K. M. Belotsky, Yu. A. Golubkov, M. Yu. Khlopov, R. V. Konoplich, and A. S. Sakharov, arXiv:astro-ph/9807027.
[38] C. Bambi and A. D. Dolgov, Nucl. Phys. **B784**, 132 (2007).
[39] V. A. Choutko, AMS days at la Palma, Spain, 2018.
[40] S. Ting, *The First Five Years of the Alpha Magnetic Spectrometer on the ISS* (2016).
[41] S. Acharya *et al.* (ALICE Collaboration), Phys. Rev. C **97**, 024615 (2018).
[42] M. di Mauro, F. Donato, A. Goudelis, and P. D. Serpico, Phys. Rev. D **90**, 085017 (2014).
[43] R. P. Duperray, K. V. Protasov, and A. Yu. Voronin, Eur. Phys. J. A **16**, 27 (2003).
[44] K. Blum, K. C. Y. Ng, R. Sato, and M. Takimoto, Phys. Rev. D **96**, 103021 (2017).
[45] J. W. Norbury and L. W. Townsend, Nucl. Instrum. Methods Phys. Res., Sect. B **254**, 187 (2007).
[46] M. Boudaud, M. Cirelli, G. Giesen, and P. Salati, J. Cosmol. Astropart. Phys. 05 (2015) 013.
[47] G. Giesen, M. Boudaud, Y. Gnolini, V. Poulin, M. Cirelli, P. Salati, and P. D. Serpico, J. Cosmol. Astropart. Phys. 09 (2015) 023.
[48] K. Hikasa *et al.* (Particle Data Group), Phys. Rev. D **45**, S1 (1992); **46**, 5210(E) (1992).
[49] A. Ghelfi, D. Maurin, A. Cheminet, L. Derome, G. Hubert, and F. Melot, Adv. Space Res. **60**, 833 (2017).
[50] Y. Gnolini *et al.*, Phys. Rev. Lett. **119**, 241101 (2017).
[51] A. Kounine (AMS Collaboration), in *Proceedings, 32nd International Cosmic Ray Conference (ICRC 2011): Beijing, China, 2011*, Vol. 12, p. 5.
[52] M. Korsmeier, F. Donato, and N. Fornengo, Phys. Rev. D **97**, 103011 (2018).
[53] F. Donato, N. Fornengo, D. Maurin, and P. Salati, Phys. Rev. D **69**, 063501 (2004).
[54] M. C. Lemaire, S. Nagamiya, S. Schnetzer, H. Steiner, and I. Tanihata, Phys. Lett. **85B**, 38 (1979).
[55] D.-M. Gomez-Coral, A. Menchaca Rocha, V. Grabski, A. Datta, P. von Doetinchem, and A. Shukla, Phys. Rev. D **98**, 023012 (2018).
[56] O. Adriani *et al.* (PAMELA Collaboration), Astrophys. J. **818**, 68 (2016).
[57] P. A. R. Ade *et al.* (Planck Collaboration), Astron. Astrophys. **594**, A13 (2016).
[58] A. Arbey, Comput. Phys. Commun. **183**, 1822 (2012).
[59] C. Pitrou, A. Coc, J.-P. Uzan, and E. Vangioni, Phys. Rep. **04**, 005 (2018).
[60] N. Padmanabhan and D. P. Finkbeiner, Phys. Rev. D **72**, 023508 (2005).
[61] A. V. Belikov and D. Hooper, Phys. Rev. D **80**, 035007 (2009).
[62] M. Cirelli, F. Iocco, and P. Panci, J. Cosmol. Astropart. Phys. 10 (2009) 009.
[63] G. Huetsi, A. Hektor, and M. Raidal, Astron. Astrophys. **505**, 999 (2009).
[64] T. R. Slatyer, N. Padmanabhan, and D. P. Finkbeiner, Phys. Rev. D **80**, 043526 (2009).
[65] A. Natarajan and D. J. Schwarz, Phys. Rev. D **78**, 103524 (2008).
[66] A. Natarajan and D. J. Schwarz, Phys. Rev. D **80**, 043529 (2009).
[67] A. Natarajan and D. J. Schwarz, Phys. Rev. D **81**, 123510 (2010).
[68] M. Valdes, C. Evoli, and A. Ferrara, Mon. Not. R. Astron. Soc. **404**, 1569 (2010).
[69] C. Evoli, M. Valdes, A. Ferrara, and N. Yoshida, Mon. Not. R. Astron. Soc. **422**, 420 (2012).
[70] S. Galli, T. R. Slatyer, M. Valdes, and F. Iocco, Phys. Rev. D **88**, 063502 (2013).
[71] D. P. Finkbeiner, S. Galli, T. Lin, and T. R. Slatyer, Phys. Rev. D **85**, 043522 (2012).
[72] G. Hutsi, J. Chluba, A. Hektor, and M. Raidal, Astron. Astrophys. **535**, A26 (2011).
[73] T. R. Slatyer, Phys. Rev. D **87**, 123513 (2013).
[74] G. Giesen, J. Lesgourgues, B. Audren, and Y. Ali-Haïmoud, J. Cosmol. Astropart. Phys. 12 (2012) 008.

[75] S. Galli, T. R. Slatyer, M. Valdes, and F. Iocco, Phys. Rev. D **88**, 063502 (2013).
[76] T. R. Slatyer, Phys. Rev. D **93**, 023527 (2016).
[77] L. Lopez-Honorez, O. Mena, S. Palomares-Ruiz, and A. C. Vincent, J. Cosmol. Astropart. Phys. 07 (2013) 046.
[78] V. Poulin, P. D. Serpico, and J. Lesgourgues, J. Cosmol. Astropart. Phys. 12 (2015) 041.
[79] H. Liu, T. R. Slatyer, and J. Zavala, Phys. Rev. D **94**, 063507 (2016).
[80] P. Stöcker, M. Krämer, J. Lesgourgues, and V. Poulin, J. Cosmol. Astropart. Phys. 03 (2018) 018.
[81] J. Chluba, Mon. Not. R. Astron. Soc. **436**, 2232 (2013).
[82] N. Aghanim *et al.* (Planck Collaboration), arXiv:1807.06209.
[83] T. R. Slatyer and C.-L. Wu, Phys. Rev. D **95**, 023010 (2017).
[84] V. Poulin, J. Lesgourgues, and P. D. Serpico, J. Cosmol. Astropart. Phys. 03 (2017) 043.
[85] C. Weniger, J. Cosmol. Astropart. Phys. 08 (2012) 007.
[86] T. Bringmann and C. Weniger, Phys. Dark Universe **1**, 194 (2012).
[87] M. Ackermann *et al.* (Fermi-LAT Collaboration), Phys. Rev. D **88**, 082002 (2013).
[88] M. Ackermann *et al.* (Fermi-LAT Collaboration), Phys. Rev. D **91**, 122002 (2015).
[89] A. A. Abdo *et al.* (Fermi-LAT Collaboration), Astrophys. J. **712**, 147 (2010).
[90] J. Aleksic *et al.* (MAGIC Collaboration), J. Cosmol. Astropart. Phys. 06 (2011) 035.
[91] A. Geringer-Sameth and S. M. Koushiappas, Phys. Rev. Lett. **107**, 241303 (2011).
[92] E. Aliu *et al.* (VERITAS Collaboration), Phys. Rev. D **85**, 062001 (2012); **91**, 129903(E) (2015).
[93] I. Cholis and P. Salucci, Phys. Rev. D **86**, 023528 (2012).
[94] M. Ackermann *et al.* (Fermi-LAT Collaboration), Phys. Rev. D **89**, 042001 (2014).
[95] A. Albert *et al.* (DES and Fermi-LAT Collaborations), Astrophys. J. **834**, 110 (2017).
[96] Yu. A. Golubkov and M. Yu. Khlopov, Yad. Fiz. **64**, 1904 (2001) [Phys. At. Nucl. **64**, 1821 (2001)].
[97] A. A. Abdo *et al.* (Fermi-LAT Collaboration), Phys. Rev. Lett. **104**, 101101 (2010).
[98] M. Ackermann *et al.* (Fermi-LAT Collaboration), Astrophys. J. **799**, 86 (2015).
[99] C. Amsler, Rev. Mod. Phys. **70**, 1293 (1998).
[100] K. M. Ferriere, Rev. Mod. Phys. **73**, 1031 (2001).
[101] O. Adriani *et al.* (PAMELA Collaboration), Science **332**, 69 (2011).
[102] F. Acero *et al.* (Fermi-LAT Collaboration), Astrophys. J. Suppl. Ser. **218**, 23 (2015).
[103] J. Knodlseder *et al.*, Astron. Astrophys. **441**, 513 (2005).
[104] G. Weidenspointner *et al.*, ESA Spec. Publ. **622**, 25 (2007).
[105] G. Weidenspointner, G. Skinner, P. Jean, J. Knödlseder, P. von Ballmoos, G. Bignami, R. Diehl, A. W. Strong, B. Cordier, S. Schanne, and C. Winkler, Nature (London) **451**, 159 (2008).
[106] D. Hooper and L. Goodenough, Phys. Lett. B **697**, 412 (2011).
[107] D. Hooper and T. Linden, Phys. Rev. D **84**, 123005 (2011).
[108] K. N. Abazajian and M. Kaplinghat, Phys. Rev. D **86**, 083511 (2012); **87**, 129902(E) (2013).
[109] T. Daylan, D. P. Finkbeiner, D. Hooper, T. Linden, S. K. N. Portillo, N. L. Rodd, and T. R. Slatyer, Phys. Dark Universe **12**, 1 (2016).
[110] F. Calore, I. Cholis, and C. Weniger, J. Cosmol. Astropart. Phys. 03 (2015) 038.
[111] M. Ajello *et al.* (Fermi-LAT Collaboration), Astrophys. J. **819**, 44 (2016).
[112] M. Aguilar *et al.* (AMS Collaboration), Phys. Rev. Lett. **117**, 091103 (2016).
[113] I. Cholis, D. Hooper, and T. Linden, Phys. Rev. D **95**, 123007 (2017).
[114] I. Cholis, D. Hooper, and T. Linden, Phys. Rev. D **93**, 043016 (2016).
[115] A. Dolgov and J. Silk, Phys. Rev. D **47**, 4244 (1993).
[116] S. I. Blinnikov, A. D. Dolgov, and K. A. Postnov, Phys. Rev. D **92**, 023516 (2015).
[117] F. Mottez and P. Zarka, Astron. Astrophys. **569**, A86 (2014).
[118] C. Badenes and D. Maoz, Astrophys. J. **749**, L11 (2012).
[119] F. Balestra *et al.*, Phys. Lett. **165B**, 265 (1985).
[120] M. D'Angelo, P. Blasi, and E. Amato, Phys. Rev. D **94**, 083003 (2016).
[121] P. von Ballmoos, Hyperfine Interact. **228**, 91 (2014).
[122] D. Tseliakhovich and C. Hirata, Phys. Rev. D **82**, 083520 (2010).
[123] M. Yu. Khlopov, R. V. Konoplich, R. Mignani, S. G. Rubin, and A. S. Sakharov, Astropart. Phys. **12**, 367 (2000).
[124] I. Affleck and M. Dine, Nucl. Phys. **B249**, 361 (1985).
[125] B. J. Carr and S. W. Hawking, Mon. Not. R. Astron. Soc. **168**, 399 (1974).
[126] B. J. Carr, Astrophys. J. **201**, 1 (1975).